

ANALYSIS



Cite this: *Energy Environ. Sci.*, 2017, 10, 1874

Environmental analysis of perovskites and other relevant solar cell technologies in a tandem configuration†

Ilke Celik,^a Adam B. Phillips,^b Zhaoning Song,^b Yanfa Yan,^b Randy J. Ellingson,^b Michael J. Heben^b and Defne Apul^b*^a

Future high performance PV devices are expected to be tandem cells consisting of a low bandgap bottom cell and a high bandgap top cell. In this study, we developed a cradle-to-end of use life cycle assessment model to evaluate the environmental impacts, primary energy demand (PED), and energy payback time (EPBT) of four integrated two-terminal tandem solar cells composed of either Si bottom and lead-based perovskite (PK_{Pb}) top cells (Si/PK_{Pb}), copper indium gallium selenide (CIGS) and PK_{Pb} (CIGS/PK_{Pb}), copper zinc tin selenide (CZTS) and PK_{Pb} (CZTS/PK_{Pb}), or tin-lead based perovskite (PK_{Sn,Pb}) and PK_{Pb} (PK_{Sn,Pb}/PK_{Pb}). Environmental impacts from single junction Si solar cells were used as a reference point to interpret the results. We found that the environmental impacts for a 1 m² area of a cell were largely determined by the bottom cell impacts and ranged from 50% (CZTS/PK_{Pb}) to 120% of those of a Si cell. The ITO layer used in Si/PK_{Pb}, CZTS/PK_{Pb}, and PK_{Sn,Pb}/PK_{Pb} is the most impactful after the Si and CIGS absorbers, and contributed up to 70% (in PK_{Sn,Pb}/PK_{Pb}) of the total impacts for these tandem PVs. Manufacturing a single two-terminal device was found to be a more environmentally friendly option than manufacturing two constituent single-junction cells and can reduce the environmental impacts by 30% due to the exclusion of extra glass, encapsulation, front contact and back contact layers. PED analysis indicated that PK_{Sn,Pb}/PK_{Pb} manufacturing has the least energy-intensive processing, and the EPBTs of Si/PK_{Pb}, CIGS/PK_{Pb}, CZTS/PK_{Pb}, and PK_{Sn,Pb}/PK_{Pb} tandems were found to be ~13, ~7, ~2, and ~1 months, respectively. On an impacts per kW h of Si basis the environmental impacts of all the devices were much higher (up to ~10 times). These results can be attributed to the low photoconversion efficiency (PCE) and short lifetime that were assumed. While PK_{Sn,Pb}/PK_{Pb} has higher impacts than Si based on current low PCE (21%) and short lifetime (5 years) assumptions, it can outperform Si if its lifetime and PCE reach 16 years and 30%, respectively. Among the configurations considered, the PK_{Sn,Pb}/PK_{Pb} structure has the potential to be the most environmentally friendly technology.

Received 14th June 2017,
Accepted 25th July 2017

DOI: 10.1039/c7ee01650f

rs.c.li/ees

Broader context

The use of photovoltaic (PV) electricity has been growing at a 30–40% rate over the past fifteen years. The adoption rate could be increased further if the technology could be made more economically viable. Two-terminal tandem solar cells, formed by monolithically integrating two single junction solar cells constructed with different band gap absorbers, offer one possible avenue for improving the photoconversion efficiency (PCE) of PV devices. However, viable routes toward high efficiency, low-cost tandems have only become available recently with the advent of a high-efficiency organo-metal halide perovskite solar cell. Options of interest include tandems constructed with a wide band gap lead based perovskite (PK_{Pb}) top cell and a low band gap bottom cell consisting of mono-crystalline silicon (Si), copper indium gallium selenide (CIGS), copper zinc tin selenide (CZTS), or tin-lead based perovskite (PK_{Sn,Pb}) devices. In this study, we used life cycle assessment (LCA) to evaluate the environmental trade-offs associated with these four leading two-terminal tandem designs. The results demonstrate that the environmental impacts of monolithically integrated two-terminal tandem devices are up to 30% less than the impact associated with the fabrication of two single-junction devices from the constituent materials. Si/PK_{Pb} has the highest environmental impacts, while CZTS/PK_{Pb} and PK_{Sn,Pb}/PK_{Pb} have the lowest impacts. With a higher PCE and comparable lifetime of state-of-the-art devices, the PK_{Sn,Pb}/PK_{Pb} tandem was found to be the most promising PV technology for lowering the environmental impacts from solar PV.

^a School of Solar and Advanced Renewable Energy, Department of Civil Engineering, University of Toledo 2801 W. Bancroft St., Toledo, OH 43606, USA.
E-mail: defne.apul@utoledo.edu

^b School of Solar and Advanced Renewable Energy, Wright Center for Photovoltaics Innovation and Commercialization, Department of Physics and Astronomy, University of Toledo 2801 W. Bancroft St., Toledo, OH 43606, USA

† Electronic supplementary information (ESI) available. See DOI: 10.1039/c7ee01650f

1. Introduction

After decades of development, photovoltaic (PV) solar cells have become an economically viable means to generate electricity for homes, transportation, and industries. In sunny regions, the levelized cost of electricity (LCOE) of commercial PV modules made from mono/and poly-crystalline silicon (Si), or thin-film technology such as CdTe and CuInGaSe₂ (CIGS) (6 to 9 ¢ per kW h) can now compete with electricity generation from conventional fossil (7 to 15 ¢ per kW h) and nuclear power plants (10 to 13 ¢ per kW h).¹ Widespread adoption of PV requires a LCOE comparable to conventional power generation sources,^{2,3} even in locations with limited solar insolation. The requirements for a low LCOE are high photoconversion efficiencies (PCEs), low manufacturing and maintenance costs, and long lifetimes with stable operation. Although current Si, CdTe, and CIGS technologies are continuously being improved and have reached PCEs in the range of 22–25%,⁴ the PCE of single-junction solar cells is restricted by the thermodynamic Shockley–Queisser limit of ~33%.⁵ With the goal of pushing PCEs to higher values, increasing effort is being directed toward developing low-cost integrated two-terminal tandem solar cells.^{6,7}

Multijunction solar cells have mainly been constructed in the crystalline III–V system (e.g., GaInP and GaInAs),⁸ the amorphous Group IV system (e.g., amorphous Si),⁹ and with organic polymers.¹⁰ However, these tandem PV technologies are not likely to be used on large scales. The III–V tandems have been limited to aerospace and concentrator PVs due to the high costs of materials and manufacturing methods. In contrast, amorphous and organic tandems can be produced at very low cost by roll-to-roll processes but suffer from relatively low PCEs (10–13%).⁴

The emergence of hybrid organic–inorganic perovskite materials has altered the tandem landscape.¹¹ With good device performance and easily varied band gaps, integrating perovskite solar cells into commercially established bottom cell technology is of great interest. Several different tandem designs composed of a wide bandgap perovskite top cell and a lower bandgap bottom cell have been reported. To construct perovskite tandem solar cells, the top perovskite cell, typically made of methylammonium lead halide perovskite (CH₃NH₃PbBr_xI_{3-x}), referred to here as PK_{Pb}, is integrated with a bottom cell composed of crystalline Si,^{12–18} CIGS,^{19–22} Cu₂ZnSn(S,Se)₄ (CZTS),²³ polymers,²⁴ or another lower bandgap perovskite (CH₃NH₃(Sn,Pb)I₃, i.e., PK_{Sn,Pb}).^{25,26} While the crystalline Si bottom cell is the only commercially established low bandgap bottom cell, the others are also of interest based on the tunability of the perovskite top cell for bandgap optimization, and on their potential for low cost manufacturing.²⁷ Though the first tandem device involving a perovskite top cell was published recently in 2014,²⁸ such devices have already demonstrated PCEs > 23%.¹⁷

Despite the clear interest in developing these devices, the environmental impacts of tandem perovskite PV cells have largely been ignored. To date, there are only two life cycle assessment (LCA) studies on tandem devices and both of these focus on the same Si/PK_{Pb} design.^{29,30} Our effort builds on these two studies and expands the analysis of the environmental impacts to encompass three other low bandgap materials that

may enable low cost production of high PCE tandem devices. A comparison between the analyses offers insight into the benefits and drawbacks of each approach. The present study also addresses the important question of whether constructing a tandem cell is indeed more environmentally preferable than having two constituent single junction cells to form a four-terminal tandem cell. We analyze this question by showing the trade-offs between higher impacts resulting from additional materials and processing steps and additional materials and lower impacts resulting from higher PCEs. Because tandem cells are still in development, and their lifetime and PCEs are still largely unknown, a sensitivity analysis was conducted to determine at which values tandem cells would have lower environmental impacts than commercial technologies.

2. Methodology

2.1 Goal and scope

The LCA models, including the inventories for material extraction, manufacturing and use phases of PV devices, were created to assess the potential environmental impact for each of the four tandem cell configurations. All of the cell architectures were modeled on high performance experimental devices reported in the literature that provided sufficient data to allow the material mass and deposition and fabrication methods to be determined.^{20,26,31,32} The impacts from the materials, electricity use, and waste were collected from the literature. The full inventory is given in Table S1 to S7 (ESI†).

The LCA models were built for 1 m² area of the cell using the GaBi Thinkstep (v.28) software. The EcoInvent v.3.0 database³³ and literature data were used for the life cycle inventory. The “Tool for Reduction and Assessment of Chemical and other environmental Impacts” (TRACI 2.0) model was used for the life cycle impact assessment (LCIA) method.³⁴ The GaBi output was exported to excel and TRACI impacts were evaluated for 1 kW h of energy generation from the PV cells. To convert impacts from 1 m² of processed cell to 1 kW h of electricity, PCE, lifetime, performance ratio, and annualized solar insolation (1700 kW h m⁻² year⁻¹) data are needed (see eqn (1) in ref. 35). PCE values were taken from the modeled PV structures (6% for CZTS/PK_{Pb},³¹ 19.5% for CIGS/PK_{Pb},²⁰ 21% for Si/PK_{Pb},³² and 21%²⁶ for PK_{Sn,Pb}/PK_{Pb}). The lifetime of established PV cells (c-Si and CIGS) is often estimated to be 30 years.³⁶ For CZTS and perovskite cells, reliable lifetime information does not currently exist, and values of 1, 2, 5, 15 and 30 years have been used in the literature.^{37–40} When two cells are in tandem, we assumed that the lifetime is the minimum value of the two cells. Initially, we assumed that the lifetime for the tandem cells is limited to 5 years due to the lifetime of the perovskite cell, but longer lifetimes were also considered in a sensitivity analysis (*vide infra*).

The TRACI method used in LCIA includes 10 environmental impact categories each of which were calculated for CZTS/PK_{Sn}, CIGS/PK_{Sn}, Si/PK_{Sn}, and PK_{Sn,Pb}/PK_{Pb} tandem cells. The impacts were then normalized to the impacts for monocrystalline Si.³⁵

This is an appropriate point of reference to enable clear comparison of tandem results with industry standard terrestrial PV technology: monocrystalline Si is currently one of the most established PV technologies.³⁷ Additionally, this technology has higher environmental impacts than other commercial PVs. This implies that a new technology is expected to at least outperform Si to be competitive in environmental impacts. A sensitivity analysis was done to analyze the effects of PCE and lifetime on environmental impacts. Variability associated with material selection for the perovskite top layers was also evaluated.

2.2 Device structures

The four architectures analyzed are shown in Fig. 1. The structures were directly taken from reported results in the literature (Si/PK_{Pb},³² CIGS/PK_{Pb},²⁰ CZTS/PK_{Pb},³¹ PK_{Sn,Pb}/PK_{Pb}²⁶). As is seen, the structures include a wide-range of materials. As depicted in Fig. 1a, the bottom cell of the Si/PK_{Pb} structure consists of Ag/In₂O₃:SnO₂(ITO)/n-type a-Si/intrinsic a-Si/Si/intrinsic a-Si/p a-Si; the tunnel junction (TJ) for the cell is ZnO:In, and the content of the top cell is PCBM/PK_{Pb}/Spiro-OMeTAD/MoO₃/ITO/Encapsulation. Fig. 1b shows that the bottom cell of CIGS/PK_{Pb} is Glass/Mo/CIGS/CdS; the TJ of the device is ZnO/ZnO:Al; and the top cell is made up of MoO₃/Spiro-OMeTAD/PK_{Pb}/TiO₂/SnO₂:F(FTO)/Encapsulation. Fig. 1c shows that the bottom cell is made up with Glass/Mo/CZTS/CdS; the TJ of the device is ITO, and the top cell includes PEDOT:PSS/PK_{Pb}/PCBM/Al/Encapsulation. Finally, the top cell includes Glass/ITO/NiO/PK_{Pb}/PCBM/ITO, the TJ of ITO, and the bottom cell of the PK_{Sn,Pb}/PK_{Pb} structure is PEDOT:PSS/PK_{Sn,Pb}/PCBM/Ag/encapsulation.

To build the LCA models here, the total inventory of materials, waste, and required energy for each layer was scaled up from the device reported in the literature to a 1 m² cell with 65% active area^{39,40} following our previous work.³⁷ Briefly, the materials and waste for small area devices were determined from the literature or personal experience and scaled up linearly with device area. The electricity inventories for small area devices were taken from

the literature and scaled up utilizing an appropriate use factor, which measures the efficiency of each deposition method, from Garcia *et al.*⁴¹

2.3 Energy requirement

Two major categories of energy consumption involved in the manufacturing of solar cells are (i) the energy embedded in the materials, and (ii) the direct processing energy used during manufacturing of the cells. The energy embedded in the materials includes all the energy involved during a material's extraction/mining from the environment, and its refinement for use in the cell.⁴² These data were taken directly from the Ecoinvent v3.1 database.⁴³ The direct processing energy, on the other hand, is specific to the materials and methods used to fabricate the cells. The deposition methods for each layer were taken from the studies that created the tandem cells.^{20,26,31,32} The direct electricity requirements for creating each layer were compiled from the literature (Table S1, ESI†)

Table 1 shows the direct energy consumption to deposit the PV layers. Vacuum-based deposition techniques (*e.g.*, sputtering and thermal evaporation) require a pumping process prior to the deposition. A non-vacuum process (*e.g.*, spin coating) is commonly followed by a post-deposition annealing process. The electricity consumption data were extracted from Garcia-Valverde *et al.*⁴¹ The energy consumption of each process was multiplied by system use factors. The use factor gives a realistic approximation based on measurements on small pieces deposited in the labs that may be used to extrapolate to mass production in the industry.⁴¹ The system use factors for the evaporator (0.64%), heater (0.2%), vacuum pump (10%) and spin coater (0.15%) were taken from the literature.⁴¹

The material-embedded and direct processing energies were used to calculate the primary energy demand (PED). PED refers to the initial forms of the energy source such as fossil fuels (coal and natural gas), biofuels, waves, winds, and solar radiation that has not been converted to a secondary form of energy, *i.e.* electricity. The conversion rate of PED to electricity varies depending on the selected grid. For example, the UCTE (Union for the Coordination of

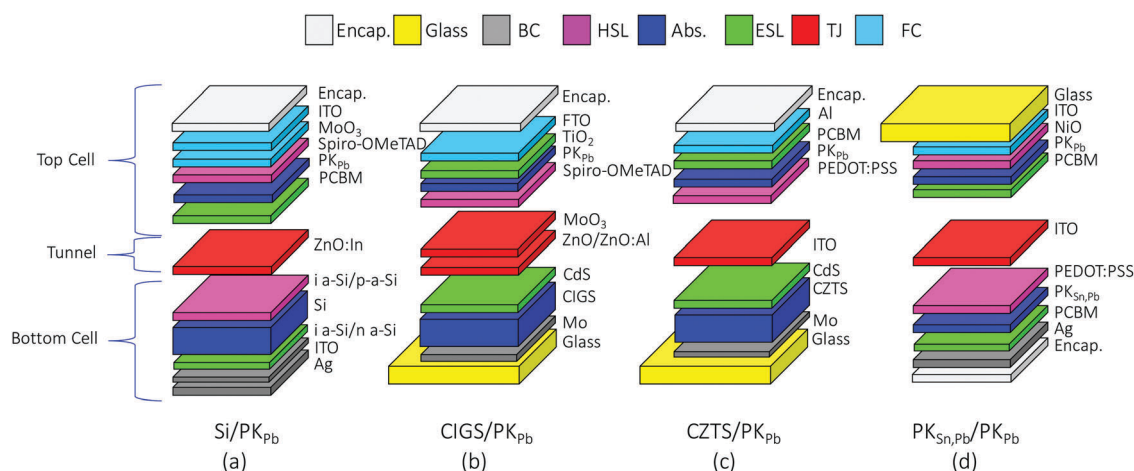


Fig. 1 Structures of two-terminal tandem (a) Si/PK_{Pb},³² (b) CIGS/PK_{Pb},²⁰ (c) CZTS/PK_{Pb}³¹ and (d) PK_{Sn,Pb}/PK_{Pb}²⁶ devices. The color coding used to indicate encapsulation (Encap), glass, back contact (BC), hole selective layer (HSL), Absorber (Abs.), electron selective layer (ESL), tunnel junction (TJ), and front contact (FC) is the same for the rest of the study.

Table 1 Direct processing energy used for depositing the PV layers of the tandem devices. The individual PV layers are categorized by their role in the cell structure. The "absorber materials" include CIGS, CZTS, Si, and both top and bottom perovskites. "Contact" includes both back (BC) and front (FC) contacts. "Charge selective" consists of electron and hole selective layers. "Others" includes the direct energy required to clean the glass substrate and encapsulation

		Cell structure (in Fig. 1)	Deposition method	Dep. time and energy	Annealing time and energy	Pumping time and energy	Use factor (%)	Electricity (MJ m ⁻²)	Remarks/source
Absorber	CIGS	B	Co-evaporation					3.30×10^2	43
	CZTS	C	Spinning, annealing	5 min 36 360 MJ	30 min 352 MJ		0.2	4.89×10	Annealing @540 °C ^d
	PK _{Pb}	All	Spinning, annealing	1 min 36 360 MJ	60 min 64.8 MJ		0.2	1.04×10	Annealing @100 °C ^d
	PK _{Sn,Pb} Si wafer	D A	Spinning, annealing Float zone growth					7.73×10^{-1} 8.81×10^2	42 and 45 43
Contact	Al ^c	C	Thermal evaporation	20 min 138 MJ		25 min 96 MJ	0.64	8.33×10^{-1}	42
	Ag ^c	a and d	Thermal evaporation	20 min 138 MJ		25 min 96 MJ	0.64	1.13×10	42
	FTO ITO ^a	B a, c and d	Screening, sintering Sputtering	8 min 118 MJ		13 min 132 MJ	10	5.53×10 1.94×10^1	39 42
	Mo	b and c	Sputtering	23 min 118 MJ		28.2 min 132 MJ	10	6.19×10^1	42
	ZnO:In	A	Sputtering	6 min 118 MJ		11 min 132 MJ	10	1.26×10^1	42
	ZnO/ZnO:Al	B	Sputtering	6.5 min 118 MJ		11.5 min 132 MJ	10	1.34×10^1	42
Charge selective	CdS	b and c	Chemical bath					8.42×10^{-2}	46
	i-aSi, n-aSi, and p-aSi NiO	A	PECVD					2.37×10	47
		D	Spinning, annealing	1 min 36 360 MJ	60 min 194 MJ		0.2	9.98×10^{-1}	Annealing @300 °C ^d
	MoO ₃ ^c	a and b	Thermal evaporation	2 min 276 MJ		7 min 96 MJ		5.96×10^{-1}	42
	PCBM	a, c and d	Spinning, annealing	1 min 36 360 MJ	10 min 45 MJ		0.2	9.24×10^{-1}	Annealing @70 °C ^d
	PEDOT:PSS	C	Spinning, annealing	1 min 36 360 MJ	15 min 78 MJ		0.2	9.48×10^{-1}	Annealing @120 °C ^d
	Spiro-OMeTAD	a and b	Spinning, annealing	1 min 36 360 MJ	10 min 45 MJ		0.2	9.22×10^{-1}	Annealing @70 °C ^d
TiO ₂ ^b	B	Spinning, annealing	1 min 36 360 MJ	75 min 292 MJ 324 MJ		0.2	1.67×10	Annealing @450 °C ^d @500 °C ^d	
Others	Glass cleaning	b-d	Sonication					2.53×10	41
	Encapsulate	All	Encapsulation					4.31×10	48

^a Electricity consumption value given for ITO, corresponds to a 110 nm ITO layer used in structure a. The electricity consumption for the ITO layers in c and d varies due to the difference in thickness (the corresponding values can be found in the ESI). ^b TiO₂ requires two-step annealing, including 45 min @450 °C and 30 min @500 °C. ^c 30 minutes of cooling time is required for Al, Ag and MoO₃ and the power consumption of the cooler is 57.6 MJ m⁻². ^d Power consumption of heaters varies linearly based on the specific temperatures given in the last column.

the Transmission of Electricity) electricity mix used in this study is converted into primary energy requirement with a conversion efficiency of 33% (*i.e.* 1 kW h of primary energy can supply 0.33 kW h of electrical energy). PEDs of tandem cell devices were analyzed in detail to determine the energy-intensive component of the cells. EPBT was calculated using the PED, annual insolation, PCE, and performance ratio of the modules.⁴⁴

3. Results and discussion

3.1 Effect of adding PK_{Pb} to the different bottom PV cells

The average normalized environmental impacts per m² of the tandem cells range between less than half of the impacts of a Si

cell to 20% greater (see the Average row in Table 2). These impacts are affected by the variability in impacts both in the top and bottom cells. The bottom cell impacts vary from 0.19 (for PK_{Sn,Pb}) to 1.00 (Si) while those of top cells (PK_{Pb} + TJ) vary from 0.11 to 0.45. Note that the reference point for this calculation is Si, which has an average impact of 1.00.

The four bottom cells have quite different impacts. The impacts of the PK_{Sn,Pb}(0.19) and CZTS(0.28) bottom cells are ~2–5 times lower than those of CIGS(0.69) and Si(1.00) bottoms cells. This is because PK_{Sn,Pb} and CZTS cells are manufactured by using solution based methods instead of the high-energy intensive methods used in Si and CIGS manufacturing. PK and CZTS are considered emerging technologies and other authors have also noted the low environmental impacts from these cells.^{29,35,39,49}

Table 2 Comparison of the normalized environmental impacts of single junction PV technologies to integrated two-terminal tandem counterparts on a unit area production (m^2) basis. The impacts of bottom, tandem and the difference (difference = $\text{PK}_{\text{Pb}} + \text{TJ}$) between the bottom and the tandems cells are also shown in the last three rows. Yellow coding means that the impact per m^2 is similar to that of Si, which is the reference case. Values coded light or dark indicated better performance, while orange and red indicate worse performance. The actual values of the Si impacts are shown in the last column

PV technology	CIGS/PK _{Pb}		CZTS/PK _{Pb}		PK _{Sn,Pb} /PK _{Pb}		Si/PK _{Pb}		Si [m^2]
	CIGS	PK _{Pb}	CZTS	PK _{Pb}	PK _{Sn,Pb}	PK _{Pb}	Si	PK _{Pb}	
Acidification	1.22	0.66	0.87	0.28	1.61	0.68	1.68	1	5.39E-01 [kg SO ₂ -Equiv.]
Ecotoxicity	1.02	0.97	0.62	0.53	0.61	0.12	1.19	1	7.28E+02 [CTU _e]
Eutrophication	0.97	0.77	0.52	0.26	0.89	0.22	1.36	1	7.13E-01 [kg N-Equiv.]
Global warming	0.52	0.49	0.22	0.16	0.40	0.07	1.13	1	1.49E+02 [kg CO ₂ -Equiv.]
Human health particulate	0.66	0.60	0.44	0.37	0.69	0.30	1.15	1	8.63E-02 [kg PM _{2.5} -Equiv.]
Human toxicity, cancer	0.56	0.52	0.25	0.18	0.41	0.05	1.14	1	1.09E-05 [CTU _h]
Human toxicity, non-cancer	1.14	1.10	0.64	0.51	0.82	0.11	1.26	1	3.68E-05 [CTU _h]
Ozone depletion	0.30	0.27	0.16	0.12	0.23	0.06	1.08	1	1.75E-05 [kg CFC 11-Equiv.]
Resources	0.34	0.31	0.18	0.13	0.27	0.09	1.08	1	1.98E+02 [MJ surplus energy]
Smog formation	0.53	0.50	0.28	0.22	0.45	0.14	1.12	1	6.86E+00 [kg O ₃ -Equiv.]
Average									
Bottom (Impacts/ m^2)		0.62		0.28		0.19		1.00	
PK _{Pb} + TJ (Impacts/ m^2)	0.11		0.14		0.45		0.22		
Tandem (Impacts/ m^2)	0.73		0.42		0.64		1.22		
	Most environmentally preferable				0.54<				
	More environmentally preferable				0.55-0.85				
	Neutral				0.86 - 1.14				
	Less environmentally preferable				1.15-1.44				
	Least environmentally preferable				1.45>				

The top cell impacts come from the PK_{Pb} and TJ. The lowest environmental impact of a $\text{PK}_{\text{Pb}} + \text{TJ}$ was found in CIGS/ PK_{Pb} , with a total impact of ~ 0.1 . In contrast, the impacts of the top $\text{PK}_{\text{Pb}} + \text{TJ}$ s deposited on the Si, CZTS, and $\text{PK}_{\text{Sn,Pb}}$ bottom cells are ~ 1.5 to 4.5 times higher than those of the CIGS/ PK_{Pb} top cell. The higher impacts for these cells are attributed to ITO. ITO is known to cause high environmental impact in PV cells, so using MoO_3 as the TJ in CIGS/ PK_{Pb} results in a low impact. The variation in impacts among CZTS/ PK_{Pb} , Si/ PK_{Pb} , and $\text{PK}_{\text{Sn,Pb}}/\text{PK}_{\text{Pb}}$ is a direct result of the ITO layer thickness (50 nm to 300 nm).

It is interesting to compare the environmental impacts of the bottom cell alone to the impacts of the two-terminal tandems (see the arrows in Table 2). In most cases, the differences are relatively small, on the order of 10–20%. A notable exception is the acidification impact, in which case the process of adding a PK_{Pb} cell produces an approximate $2\times$ increase. This result is due to the use of *N,N*-dimethyl formamide (DMF) used in the fabrication of the $\text{PK}_{\text{Sn,Pb}}$ layer, and is in agreement with an earlier study.³⁷ An increase in ecotoxicity impacts for $\text{PK}_{\text{Sn,Pb}}/\text{PK}_{\text{Pb}}$ (light green to red), and Si/ PK_{Pb} (yellow to red) is due to the use of ITO and ZnO:In in the top cells, respectively. An increase in eutrophication impacts of $\text{PK}_{\text{Sn,Pb}}/\text{PK}_{\text{Pb}}$ and Si/ PK_{Pb} cells is due to both the ITO and PK_{Pb} absorber layers, while that of CIGS/ PK_{Pb} is solely attributed to the PK_{Pb} layer. The changes observed in human health particulate air, and non-cancer human toxicity impact categories of $\text{PK}_{\text{Sn,Pb}}/\text{PK}_{\text{Pb}}$, and Si/ PK_{Pb} are also due to the ITO layers found in the top PK cells of these tandems. Similar changes were also observed in CZTS/ PK_{Pb} cells; however, changes regarding these impacts cannot be observed in the color coding table since the

values mostly remained in the dark green area (most environmentally preferable).

3.2 Effects of alternative contacting material

The dominance of environmental impacts from ITO is consistent with previous studies.^{35,39,41,42,50,51} The reason for high impacts is the extensive energy required to sputter the layer and the high embedded energy within the indium content of the material. ITO could be replaced by other materials such as ZnO/ZnO:Al, ZnO:In, MoO_3 , or single walled carbon nanotubes (SWCNT)⁵² to reduce environmental impacts of the devices. The effect of this possible replacement is explored in Fig. 2.

Fig. 2(a) shows that ITO (100 nm) yields more than five times the environmental impact compared to other alternative materials that can be used as the TJ and/or contacts. This is an important difference considering each device has different amounts of ITO. For example, a Si/ PK_{Pb} cell has 110 and 80 nm ITO as a FC, and a BC, respectively. CZTS/ PK_{Pb} has 50 nm ITO in the TJ, and $\text{PK}_{\text{Sn,Pb}}/\text{PK}_{\text{Pb}}$ has 100 and 200 nm in the TJ and FC, respectively. On the other hand, CIGS/PK does not include an ITO component at all. The effect of replacing the ITO in these tandem cells is shown in Fig. 2(b). The lowest end of the floating bars shows the environmental impacts of tandems that have Al contacts (the lowest impact layer among the alternatives) while the highest end of the bars shows the impacts with ITO. The black diamonds bars show the impacts of the reported tandem PVs. The results show that $\text{PK}_{\text{Sn,Pb}}/\text{PK}_{\text{Pb}}$ is the most environmentally preferable PV option among the assessed cells when the contact materials are kept the same across the different designs.

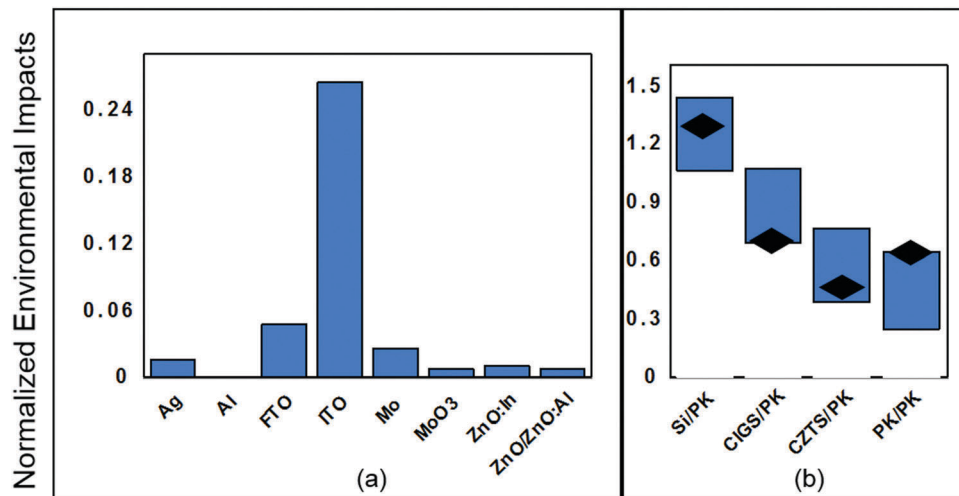


Fig. 2 The environmental impacts of alternative contacting materials (a) and the variations of the total environmental impacts of the tandems per material content (b).

3.3 Sensitivity of the kW h impacts based on PCE and lifetime

Section 3.1 showed that, except for Si/PK_{Pb}, the tandem cells presented encouraging per m² impacts (~30-to-60% lower) relative to single-junction Si PV. Yet, when impacts are calculated per unit electricity generated (Impact per kW h), the results are much less encouraging, with tandem devices having much greater impacts (5–10 times more) than that of Si (Table 3).

Impacts in /m² are converted to /kW h by dividing the value by total kW h energy generated per m² of the panel, given by eqn (1):³⁵

$$\text{Impacts}_{\text{kWh}} = \frac{\text{Impacts}_{\text{m}^2}}{I \times \text{PCE} \times \text{PR} \times \text{Lt}} \quad (1)$$

where impacts_{m²} = impact per 1 m² module area manufacturing; impacts_{kWh} = impact per kW h energy generation from PV module; *I* = solar insolation constant (kW h m⁻² year⁻¹); PR = performance ratio of the module (%); Lt = lifetime of the PV technology (year). The high values of impacts_{kWh} indicate that the panel does not generate a lot of power. This is attributed to the low PCE, and short Lt assumed for the tandem cell. The PCEs used in this life cycle environmental impact analysis are the highest reported values; however, because the technology is new, the reported PCEs are still well below the values we expect to see in the near future. Additionally, the assumed lifetimes of the emerging technologies are low right now. These combined effects greatly reduce the total power generated from the panel.

To get a better understanding of what the impacts would be as the devices improve, the impacts per kW h were determined as a function of Lt, and PCE (Fig. 3). Fig. 3a shows the average impacts of the Si/PK_{Pb} tandem device. Only a narrow window of long Lt and high PCE for the tandem would result in an impact that would be lower on average than that of a Si cell. This is because both the Lt (30 years), and PCE (25%) of Si are already high. At the same time, the impacts of the fabrication process of the top cell, while small compared to those of Si fabrication,

are non-zero with, presently, no added efficiency benefit. For a tandem device that reached the Shockley & Queisser PCE limit (40% for these two bandgaps), the shortest Lt required to match an impact of Si alone (yellow shaded area) is 20 years, while a PCE of 26.5% would be required for a Si/PK_{Pb} tandem device with 30 years of Lt.

CIGS/PK_{Pb} (Fig. 3b), CZTS/PK_{Pb} (Fig. 3c), and PK_{Sn,Pb}/PK_{Pb} (Fig. 3d) have a much wider range of Lt and PCE that could provide lower impacts than Si. To match the impacts of Si, the product of Lt and PCE needs to exceed 915 year % for Si/PK_{Pb}, 555 year % for CIGS/PK_{Pb}, 315 year % for CZTS/PK_{Pb} year %, and 480 year % for PK_{Sn,Pb}/PK_{Pb}. These values for the Lt and PCE were determined using eqn (2):

$$\frac{\text{PCE}_{\text{tandem}} \times \text{Lt}_{\text{tandem}}}{\text{Impact}_{\text{tandem}}} < \frac{\text{PCE}_{\text{Si}} \times \text{Lt}_{\text{Si}}}{\text{Impact}_{\text{Si}}} \quad (2)$$

where Impact_{tandem} and Impact_{Si} are the average environmental impacts per m² of tandem and Si module production, respectively. PCE_{Si} (25%) and Lt_{Si} (30 years) are taken from Table 3. For example, to match the impacts of a Si cell, the required PCE and Lt of the PK_{Sn,Pb}/PK_{Pb} tandem cell would be 30% and 16 years, respectively. These achievable Lts and PCE parameters suggest a bright future for PK_{Sn,Pb}/PK_{Pb} and CIGS/PK_{Pb} tandem cells. The product of Lt and PCE is even lower for CZTS/PK_{Pb} but this technology currently has a very low PCE (6%) and needs to make significant strides in PCE before it can be viewed as a promising option.

3.4 Comparing the integrated two-terminal tandem cell to two constituent single junction cells

The primary goal of manufacturing a two-terminal device instead of manufacturing two separate single junction devices (or four-terminal tandems) is to attain higher efficiencies while saving on balance of modules (*e.g.*, glass, and encapsulation) and balance of system costs (*e.g.* mounting and wiring). However, the current best-reported efficiencies of perovskite tandem

Table 3 Comparison of the normalized environmental impacts of single junction PV technologies to integrated two-terminal tandem counterparts on a unit energy generation (kW h) basis. The same color coding in Table 2 was used to categorize the impacts of the cells. Note that PCEs of CIGS, CZTS, $\text{PK}_{\text{Sn,Pb}}$ and Si were taken from the NREL best cell efficiency diagram⁴. The lifetimes (Lt) of Si and CIGS were taken from the literature⁵³

PV technology	CIGS/ PK_{Pb}	CIGS	CZTS/ PK_{Pb}	CZTS	$\text{PK}_{\text{Sn,Pb}}/\text{PK}_{\text{Pb}}$	$\text{PK}_{\text{Sn,Pb}}$	Si/ PK_{Pb}	Si	
	PCE	19.5%	22.3%	6.0%	12.3%	21.0%	16.0%	21.0%	25.0%
	Lt	5	30	5	5	5	5	5	30
Bottom (Impacts/kWh)			0.69		3.36		1.74		1.00
Tandem (Impacts/kWh)		5.58		10.43		4.57		8.71	

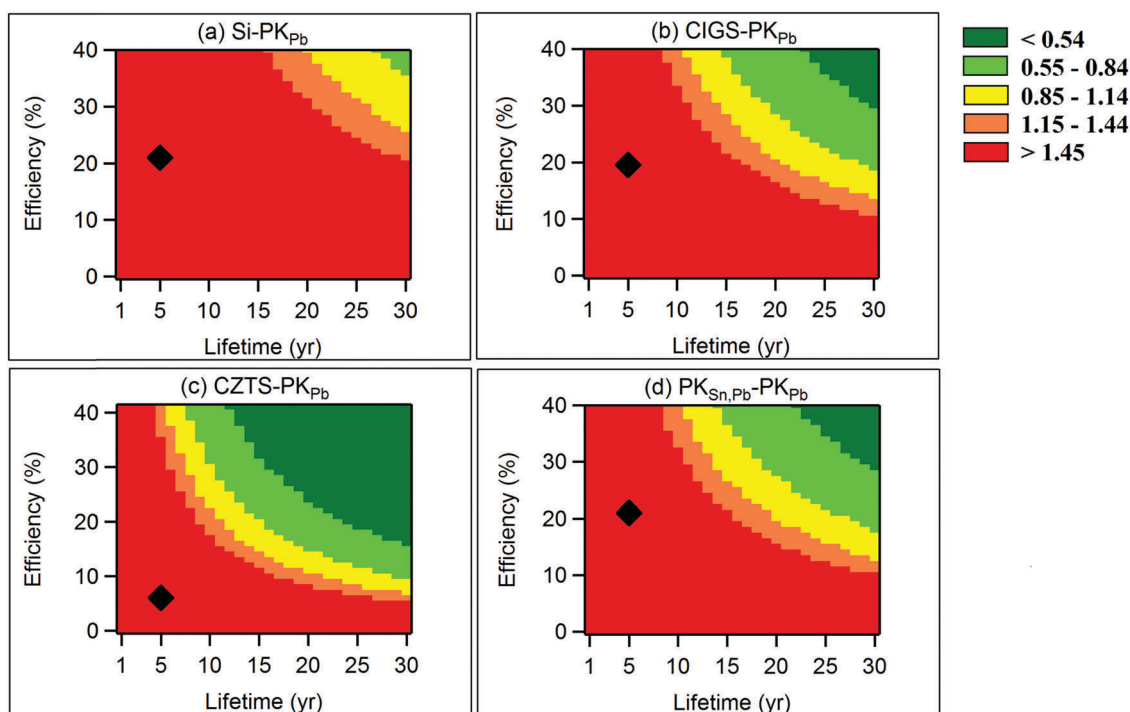


Fig. 3 The effects of PCE and lifetime (Lt) assumptions on the normalized average environmental impacts of tandem cells. This figure shows how the impacts per kW h would be affected by changes in lifetime and efficiency. Impacts corresponding to the current Lt and PCE of the tandems are shown with diamonds. The color coding used here is the same as that used in Table 2.

devices have not yet reached the PCE levels of the single cell devices. Thus, we compared the single junction and integrated two-terminal tandem structures in terms of impacts per m^2 (instead of impacts per kW h). Fig. 4 shows the environmental impacts from manufacturing of integrated two-terminal junction structures (cell 1/cell 2) and the two constituent single junction cells (cell 1 + cell 2).

In general, integrated two-terminal tandem cells have two glass layers (each ~ 2.5 mm, at the top and bottom surfaces) while the manufacturing of two separate cells leads to a total of four glass layers (two for each cell). The only exception to this is the Si/ PK_{Pb} devices, in which the Si/ PK_{Pb} tandem includes one glass layer for the module, and single-junction Si and PK_{Pb} cells require one glass substrate for Si and two glass layers for the PK_{Pb} cell (each glass layer shown in Fig. 4(b)–(d) corresponds to two layers of glass). Each two-terminal tandem cell also includes a TJ (red bars) to connect the bottom cells to top cells. The same contacting role is performed by additional FC and BC

in the individual cells. These FC and BC are assumed to be the same materials as the TJ. Also, individual cells require separate encapsulation layers while tandem cells have only one. The difference between glass, encapsulations, FC, BC, and TJs offers a trade-off between the manufacturing of two-terminal tandems and separate cells. The environmental impacts of those layers are 2.22, 2.02, 2.17, and 5.24 for Si/ PK_{Pb} , CIGS/ PK_{Pb} , CZTS/ PK_{Pb} and $\text{PK}_{\text{Sn,Pb}}/\text{PK}_{\text{Pb}}$, respectively. The environmental impact for tandem structures depends critically on the total impact advantage offered by using a TJ in place of the net material difference on the glass, encapsulation, FC, and BC layers. For example, the total environmental impacts for the Si/ PK_{Pb} and CIGS/ PK_{Pb} devices are $\sim 3.2\%$ and 7.1% lower than those impacts from separate Si and PK_{Pb} (Si + PK_{Pb}) and CIGS and PK_{Pb} (CIGS + PK_{Pb}) respectively. Similarly, the total environmental impacts for CZTS/ PK_{Pb} and $\text{PK}_{\text{Sn,Pb}}/\text{PK}_{\text{Pb}}$ are 30.1% and 27.3% lower than those from individual cells. The use of ITO as a part of front and back contacts has a significant impact on these results.

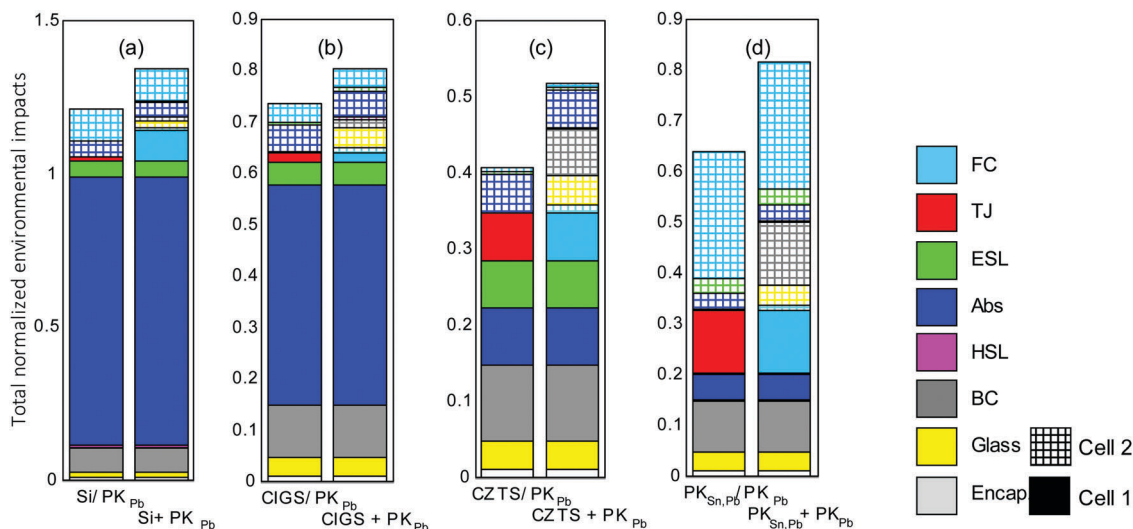


Fig. 4 Comparison of total normalized environmental impacts of single junction and two-terminal tandem devices with Si (a), CIGS (b), CZTS (c) and $\text{PK}_{\text{Sn,Pb}}$ (d) components.

It should be noted that the balance of system (BOS) composed of mounting, cabling, and inverter systems is not included in this analysis, and inclusion would likely result in even better environmental performance for the two-terminal tandem cells relative to the four-terminal device.⁵⁴ Previous LCA studies have shown that the BOS contributes to 25–30% of the total impacts of a PV module, mainly due to the mounting component such as the supporting structures, boxes, and frame junction.^{50,55,56} While the mounting of the tandems is expected to be similar to that of a single junction device, two inverters would be needed for two constituent single junction modules. Because this is excluded from these cells, it is likely that the environmental improvements achieved using two-terminal

tandem devices are underestimated relative to two single junction devices.

3.5 PED and EPBT analysis

An analysis was conducted to determine energy input requirements of each layer in the tandem devices (Fig. 5). As in Fig. 2, the effect of ITO and its potential replacement was also captured using error bars. In general, $\text{Si}/\text{PK}_{\text{Pb}}$ has the highest average PED (3000 MJ m^{-2}) while $\text{PK}_{\text{Sn,Pb}}/\text{PK}_{\text{Pb}}$ has the lowest PED value, $\sim 15\%$ of that of $\text{Si}/\text{PK}_{\text{Pb}}$. The high PED of $\text{Si}/\text{PK}_{\text{Pb}}$ is attributed to the silicon absorber of the bottom cell which requires energy intensive processes to purify the silicon to solar grade.^{57,58} The energy requirement for these purification

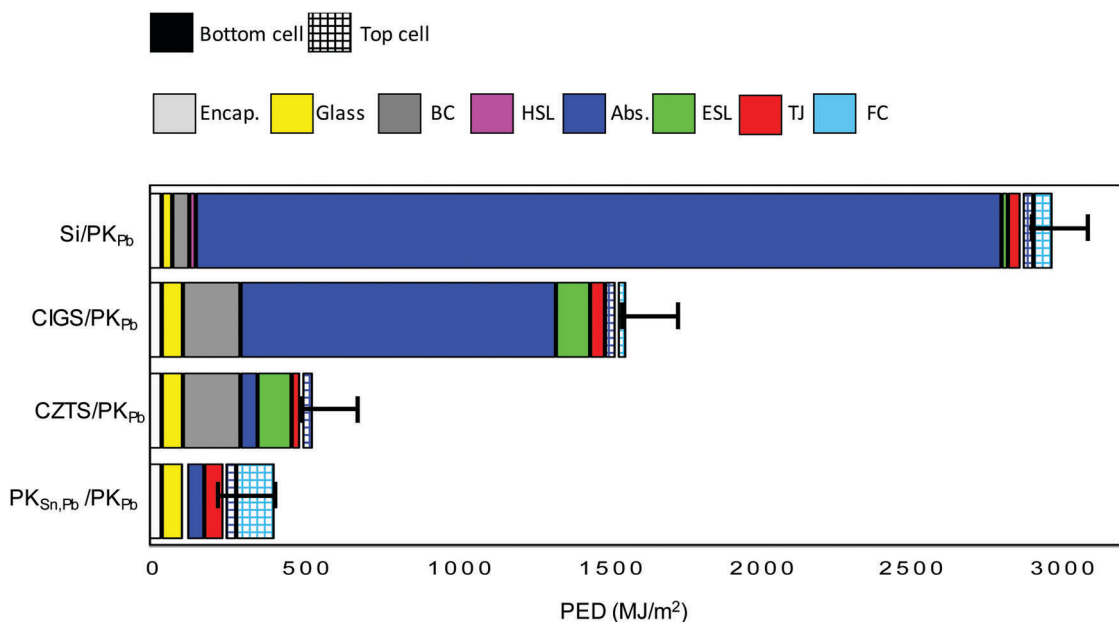


Fig. 5 PED required to manufacture tandem PV devices using perovskite as the top cell's light absorber. Solid colors are for bottom cells and squared patterns are for the top perovskite cells.

Table 4 EPBT of two-terminal tandem devices

	Si/PK _{Pb}	CIGS/PK _{Pb}	CZTS/PK _{Pb}	PK _{Sn,Pb} /PK _{Pb}
EPBT (months)	13–13.5	7–8	2–3	1–1.7

processes accounts for 90% of the total energy required for PV cell production.

The PED of CIGS/PK was found to be 1585 MJ m⁻². Similar to Si/PK_{Pb}, the absorber layer accounts for a significant portion (70%) of the energy required to fabricate the device. The high energy-intensity of the CIGS absorber is due to the high temperature processing to evaporate the constituents of the layer, and the high substrate temperatures required during deposition. The contributions of the Mo BC (~12%) and CdS ESL (~7%) to the PED of the CIGS/PK_{Pb} device are also significant. The PEDs of CZTS/PK_{Pb} (549 MJ m⁻²) and PK_{Sn,Pb}/PK_{Pb} (419 MJ m⁻²) are about three times lower than those of CIGS/PK_{Pb} and six times lower than those of Si/PK_{Pb}. The Mo BC dominates the PED breakdown (34%) of the CZTS/PK_{Pb} device. This is because it is deposited by sputtering, and with 600 nm, this is one of the thickest layers in the device. The energy-intensive profile of the Mo BC is consistent with that in the literature.^{46,59} The PED breakdown of the PK_{Sn,Pb}/PK_{Pb} device is a little more evenly divided among the FC, absorbers, TJ, and encapsulation which accounts for 30, 25, 16, and 13% the total PED, respectively.

As shown in eqn (3), PED information can be used to estimate the EPBT, which is the time needed for the solar cell to generate the equivalent energy consumed during manufacturing of the PV modules:^{44,60}

$$\text{EPBT} = \frac{\text{PED} \times \varepsilon}{I \times \eta \times \text{PR} \times \text{CF}} \quad (3)$$

where PED is the primary energy demand (MJ_{primary} m⁻²), ε is the electrical to primary energy conversion factor (35%), PR is the performance ratio (%), η is the PCE (%), I is the insolation constant (kW h m⁻² year⁻¹), and CF is the conversion factor (3.6 MJ kW⁻¹ h⁻¹). This analysis shows that PK_{Sn,Pb}/PK_{Pb} is expected to have the lowest EPBT (~1 month) among the tandem devices considered in this study (Table 4). Note that the current PCE of tandem devices is around 50% of the SQL of two-terminal devices; thus, further reductions are possible with increasing PCE improvements.

4. Conclusions

A cradle-to-end of use life cycle analysis was conducted to evaluate the environmental impacts, PED, and EPBT of four tandem perovskite devices having Si, CIGS, CZTS, and PK_{Sn,Pb} as bottom cells. The environmental impacts of Si were used as a reference point to interpret the results. The results show that environmental impacts per m² of PK_{Pb} top cells are much lower than those of bottom Si, CIGS, and CZTS cells; thus, the impacts at the tandem device are largely determined by the bottom cell. ITO used in Si/PK_{Pb}, CZTS/PK_{Pb}, and PK_{Sn,Pb}/PK_{Pb}

is the most impactful layer after Si and CIGS absorbers, and contributed up to 70% of the total impacts per m² of these tandem PVs. Compared to the impacts per kW h of Si, environmental impacts of all the devices are much higher (up to ~10 times higher). These results are due to the low PCE and short Lt assumed. Reasonable increases in both parameters will result in tandem cells having impacts equal to or lower than those of Si. For example, PK_{Sn,Pb}/PK_{Pb} will have a lower impact than Si if it has a minimum Lt of 16 years and PCE of 30%. In this study, we also showed that manufacturing the cells separately, instead of in a tandem structure, would considerably increase the impacts (up to 30%) due to the inclusion of extra glass, encapsulation, FC and BC layers. The PED (419–3000 MJ m⁻²) and EPBT (1–13 months) all followed the same ranking; PK_{Sn,Pb}/PK_{Pb} < CZTS/PK_{Pb} < CIGS/PK_{Pb} < Si/PK_{Pb}. While CZTS/PK_{Pb} and PK_{Sn,Pb}/PK_{Pb} were close in environmental impacts, the low PCE of CZTS/PK_{Pb} is likely to hinder deployment of this technology, leaving PK_{Sn,Pb}/PK_{Pb} as the most promising PV technology to offer lower environmental impacts from solar PVs.

Acknowledgements

This study was funded by the National Science Foundation (CHE-1230246, ECCS-1665172) and the Office of Naval Research (N00014-17-1-2223).

References

- J. Jean, P. R. Brown, R. L. Jaffe, T. Buonassisi and V. Bulovic, *Energy Environ. Sci.*, 2015, **8**, 1200–1219.
- I. Renewable Energy Agency, 2010.
- C. Bailie and M. McGehee, *MRS Bull.*, 2015, **40**, 681–686.
- NREL, 2017.
- W. Shockley and H. J. Queisser, *J. Appl. Phys.*, 1961, **32**, 510–519.
- A. De Vos, *J. Phys. D: Appl. Phys.*, 1980, **13**, 839–846.
- S. Albrecht and B. Rech, *Nat. Energy*, 2017, **2**, 16196.
- R. R. King, D. C. Law, K. M. Edmondson, C. M. Fetzer, G. S. Kinsey, H. Yoon, R. A. Sherif and N. H. Karam, *Appl. Phys. Lett.*, 2007, **90**, 183516.
- J. Yang, A. Banerjee and S. Guha, *Appl. Phys. Lett.*, 1997, **70**, 2975–2977.
- J. You, L. Dou, K. Yoshimura, T. Kato, K. Ohya, T. Moriarty, K. Emery, C.-C. Chen, J. Gao, G. Li and Y. Yang, *Nat. Commun.*, 2013, **4**, 1446.
- B. Chen, X. Zheng, Y. Bai, N. P. Padture and J. Huang, *Adv. Energy Mater.*, 2017, 1602400.
- C. D. Bailie, M. G. Christoforo, J. P. Mailoa, A. R. Bowring, E. L. Unger, W. H. Nguyen, J. Burschka, N. Pellet, J. Z. Lee, M. Grätzel, R. Noufi, T. Buonassisi, A. Salleo and M. D. McGehee, *Energy Environ. Sci.*, 2015, **8**, 956–963.
- S. Albrecht, M. Saliba, J. P. Correa Baena, F. Lang, L. Kegelman, M. Mews, L. Steier, A. Abate, J. Rappich, L. Korte, R. Schlattmann, M. K. Nazeeruddin, A. Hagfeldt, M. Grätzel and B. Rech, *Energy Environ. Sci.*, 2016, **9**, 81–88.

- 14 B. Chen, Y. Bai, Z. Yu, T. Li, X. Zheng, Q. Dong, L. Shen, M. Boccard, A. Gruverman, Z. Holman and J. Huang, *Adv. Energy Mater.*, 2016, **6**, 1601128.
- 15 D. P. McMeekin, G. Sadoughi, W. Rehman, G. E. Eperon, M. Saliba, M. T. Hörlantner, A. Haghighirad, N. Sakai, L. Korte, B. Rech, M. B. Johnston, L. M. Herz and H. J. Snaith, *Science*, 2016, **351**, 151–155.
- 16 J. Werner, C.-H. Weng, A. Walter, L. Fesquet, J. P. Seif, S. De Wolf, B. Niesen and C. Ballif, *J. Phys. Chem. Lett.*, 2016, **7**, 161–166.
- 17 K. A. Bush, A. F. Palmstrom, Z. J. Yu, M. Boccard, R. Cheacharoen, J. P. Mailoa, D. P. McMeekin, R. L. Z. Hoye, C. D. Baillie, T. Leijtens, I. M. Peters, M. C. Minichetti, N. Rolston, R. Prasanna, S. Sofia, D. Harwood, W. Ma, F. Moghadam, H. J. Snaith, T. Buonassisi, Z. C. Holman, S. F. Bent and M. D. McGehee, *Nat. Energy*, 2017, **2**, 17009.
- 18 J. Werner, L. Barraud, A. Walter, M. Bra, F. Sahli, D. Sacchetto, N. Tereault, B. Paviet-Salomon, S.-J. Moon, C. Allebe Matthieu Despeisse, S. Nicolay, S. De Wolf, B. Niesen and C. Ballif, *ACS Energy Lett.*, 2016, **1**, 474–480.
- 19 C. D. Baillie, M. G. Christoforo, J. P. Mailoa, A. R. Bowering, E. L. Unger, W. H. Nguyen, J. Burschka, N. Pellet, J. Z. Lee, M. Grätzel, R. Noufi, T. Buonassisi, A. Salleo and M. D. McGehee, *Energy Environ. Sci.*, 2014, **8**, 956–963.
- 20 L. Kranz, A. Abate, T. Feurer and F. Fu, *J. Phys. Chem. Lett.*, 2015, **6**, 2676–2681.
- 21 F. Fu, T. Feurer, T. Jäger, E. Avancini, B. Bissig, S. Yoon, S. Buecheler and A. N. Tiwari, *Nat. Commun.*, 2015, **6**, 8932.
- 22 T. Todorov, T. Gershon, O. Gunawan, Y. S. Lee, C. Sturdevant, L.-Y. Chang and S. Guha, *Adv. Energy Mater.*, 2015, **5**, 1500799.
- 23 T. Todorov, T. Gershon, O. Gunawan, C. Sturdevant and S. Guha, *Appl. Phys. Lett.*, 2014, **105**, 173902.
- 24 Y. Liu, L. A. Renna, M. Bag, Z. A. Page, P. Kim, J. Choi, T. Emrick, D. Venkataraman and T. P. Russell, *ACS Appl. Mater. Interfaces*, 2016, **8**, 7070–7076.
- 25 D. Zhao, Y. Yu, C. Wang, W. Liao, N. Shrestha, C. R. Grice, A. J. Cimaroli, L. Guan, R. J. Ellingson, K. Zhu, X. Zhao, R.-G. Xiong and Y. Yan, *Nat. Energy*, 2017, **2**, 17018.
- 26 G. E. Eperon, T. Leijtens, K. A. Bush, R. Prasanna, T. Green, J. T.-W. Wang, D. P. McMeekin, G. Volonakis, R. L. Milot, R. May, A. Palmstrom, D. J. Slotcavage, R. A. Belisle, J. B. Patel, E. S. Parrott, R. J. Sutton, W. Ma, F. Moghadam, B. Conings, A. Babayigit, H.-G. Boyen, S. Bent, F. Giustino, L. M. Herz, M. B. Johnston, M. D. McGehee and H. J. Snaith, *Science*, 2016, **354**, 861–865.
- 27 Z. Song, C. L. McElvany, A. B. Phillips, I. Celik, P. W. Krantz, S. C. Wathage, G. K. Liyanage, D. Apul and M. J. Heben, *Energy Environ. Sci.*, 2017, **10**, 1297–1305.
- 28 C. D. Baillie, M. G. Christoforo, J. P. Mailoa, A. R. Bowering, E. L. Unger, W. H. Nguyen, J. Burschka, N. Pellet, J. Z. Lee, M. Grätzel, R. Noufi, T. Buonassisi, A. Salleo and M. D. McGehee, *Energy Environ. Sci.*, 2015, **8**, 956–963.
- 29 M. Monteiro Lunardi, A. Wing Yi Ho-Baillie, J. P. Alvarez-Gaitan, S. Moore and R. Corkish, *Prog. Photovoltaics Res. Appl.*, 2017, **25**, 679–695.
- 30 M. Hauck, T. Ligthart, M. Schaap, E. Boukris and D. Brouwer, *J. Renewable Energy*, 2017, **111**, 906–913.
- 31 T. Todorov, T. Gershon and O. Gunawan, *Appl. Phys. Lett.*, 2014, **105**, 173902.
- 32 J. Werner, C.-H. Weng, A. Walter, L. Fesquet, J. P. Seif, S. De Wolf, B. Niesen and C. Ballif, *J. Phys. Chem. Lett.*, 2016, **7**, 161–166.
- 33 G. Wernet, C. Bauer, B. Steubing, J. Reinhard, E. Moreno-Ruiz and B. Weidema, *Int. J. Life Cycle Assess.*, 2016, **21**, 1218–1230.
- 34 J. Bare, *Clean Technol. Environ. Policy*, 2011, **13**, 687–696.
- 35 I. Celik, B. E. Mason, A. B. Phillips, M. J. Heben and D. S. Apul, *Environ. Sci. Technol.*, 2017, **51**, 4722–4732.
- 36 H. C. Kim, V. Fthenakis, J. K. Choi and D. E. Turney, *J. Ind. Ecol.*, 2012, **16**, S110–S121.
- 37 I. Celik, Z. Song, A. J. Cimaroli, Y. Yan, M. J. Heben and D. Apul, *Sol. Energy Mater. Sol. Cells*, 2016, **156**, 157–169.
- 38 N. Espinosa, L. Serrano-luján, A. Urbina and F. C. Krebs, *Sol. Energy Mater. Sol. Cells*, 2015, **137**, 303–310.
- 39 J. Gong, S. Darling and F. You, *Energy Environ. Sci.*, 2015, **8**, 1953–1968.
- 40 J. Zhang, X. Gao, Y. Deng, B. Li and C. Yuan, *ChemSusChem*, 2015, **8**, 3882–3891.
- 41 R. García-Valverde, J. a. Cherni and A. Urbina, *Prog. Photovoltaics Res. Appl.*, 2010, **18**, 535–538.
- 42 N. Espinosa, R. García-Valverde, A. Urbina and F. C. Krebs, *Sol. Energy Mater. Sol. Cells*, 2011, **95**, 1293–1302.
- 43 G. Wernet, C. Bauer, B. Steubing, J. Reinhard, E. Moreno-Ruiz and B. Weidema, *Int. J. Life Cycle Assess.*, 2016, **21**, 1218–1230.
- 44 K. P. Bhandari, J. M. Collier, R. J. Ellingson and D. S. Apul, *Renewable Sustainable Energy Rev.*, 2015, **47**, 133–141.
- 45 L. Serrano-Lujan, N. Espinosa, T. T. Larsen-Olsen, J. Abad, A. Urbina and F. C. Krebs, *Adv. Energy Mater.*, 2015, **5**, DOI: 10.1002/aenm.201501119.
- 46 J. Collier, S. Wu and D. Apul, *Energy*, 2014, **74**, 314–321.
- 47 A. Louwen, W. G. J. H. M. van Sark, R. E. I. Schropp, W. C. Turkenburg and A. P. C. Faaij, *Prog. Photovoltaics Res. Appl.*, 2015, **23**, 1406–1428.
- 48 N. Espinosa, R. García-Valverde, A. Urbina, F. Lenzmann, M. Manceau, D. Angmo and F. C. Krebs, *Sol. Energy Mater. Sol. Cells*, 2012, **97**, 3–13.
- 49 J. Collier, S. Wu and D. Apul, *Energy*, 2014, **74**, 314–321.
- 50 M. D. Chatzisdoris, N. Espinosa, A. Laurent and F. C. Krebs, *Sol. Energy Mater. Sol. Cells*, 2016, 1–9.
- 51 S. Lizin, S. Van Passel, E. De Schepper, W. Maes, L. Lutsen, J. Manca and D. Vanderzande, *Energy Environ. Sci.*, 2013, **6**, 3136.
- 52 A. Ramaswami, D. Boyer, A. S. Nagpure, A. Fang, S. Bogra, B. Bakshi, E. Cohen and A. Rao-Ghorpade, *Environ. Res. Lett.*, 2017, **12**, 25008.
- 53 IRENA, *End of Life Management of Photovoltaic Panels*, 2016.
- 54 A. Louwen, W. G. J. H. M. Sark, R. E. I. Schropp, W. C. Turkenburg and A. P. C. Faaij, *Prog. Photovoltaics Res. Appl.*, 2015, **23**, 1406–1428.

- 55 M. P. Tsang, G. W. Sonnemann and D. M. Bassani, *Sol. Energy Mater. Sol. Cells*, 2016, **156**, 37–48.
- 56 A. L. Roes, E. A. Alsema, K. Blok and M. K. Patel, *Prog. Photovoltaics Res. Appl.*, 2009, **17**, 372–393.
- 57 N. Jungbluth, *Prog. Photovoltaics Res. Appl.*, 2005, **13**, 429–446.
- 58 V. M. Fthenakis and H. C. Kim, *Sol. Energy*, 2011, **85**, 1609–1628.
- 59 R. P. Scott, A. C. Cullen, C. Fox-Lent and I. Linkov, *Risk Anal.*, 2016, **36**, 1916–1935.
- 60 M. Raugei, S. Bargigli and S. Ulgiati, *Energy*, 2007, **32**, 1310–1318.